Supporting Information

Multicolor High-Speed Tracking of Single Biomolecules with Silver, Gold, and Silver−Gold Alloy Nanoparticles

Jun Ando*[,†‡], Akihiko Nakamura[†,‡], Mayuko Yamamoto[†], Chihong Song[§], Kazuyoshi Murata[§], and Ryota Iino*[,†,‡]

[†]Institute for Molecular Science, National Institutes of Natural Sciences, 5-1 Higashiyama, Myodaiji, Okazaki, Aichi 444-8787, Japan

[‡]The Graduate University for Advanced Studies (SOKENDAI), Shonan Village, Hayama, Kanagawa, 240-0193, Japan

[§]National Institute for Physiological Sciences, National Institutes of Natural Sciences, 5-1 Higashiyama, Myodaiji, Okazaki, Aichi 444-8787, Japan

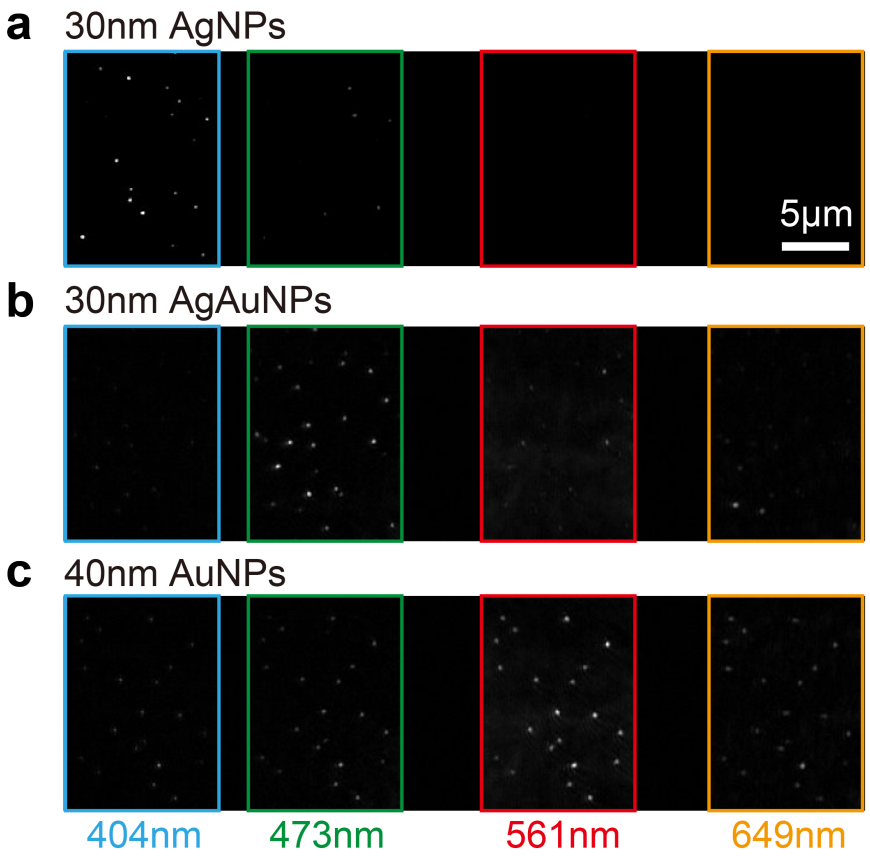

Figure S1. Dark-field images of AgNPs, AgAuNPs (5:5), and AuNPs without pixel intensity offset. (**a-c**) Dark-field images of (**a**) 30 nm AgNPs, (**b**) 30 nm AgAuNPs (5:5), and (**c**) 40 nm AuNPs. The images were taken with multiple lasers at 404 nm, 473 nm, 561 nm, and 649 nm. Laser intensities were 3.2 μW/μm^2 for 404 nm, 473 nm, and 649 nm, and 2.3 μW/μm^2 for 561 nm. The images were taken at 333 μs time resolution. Scale bar, 5 μm.

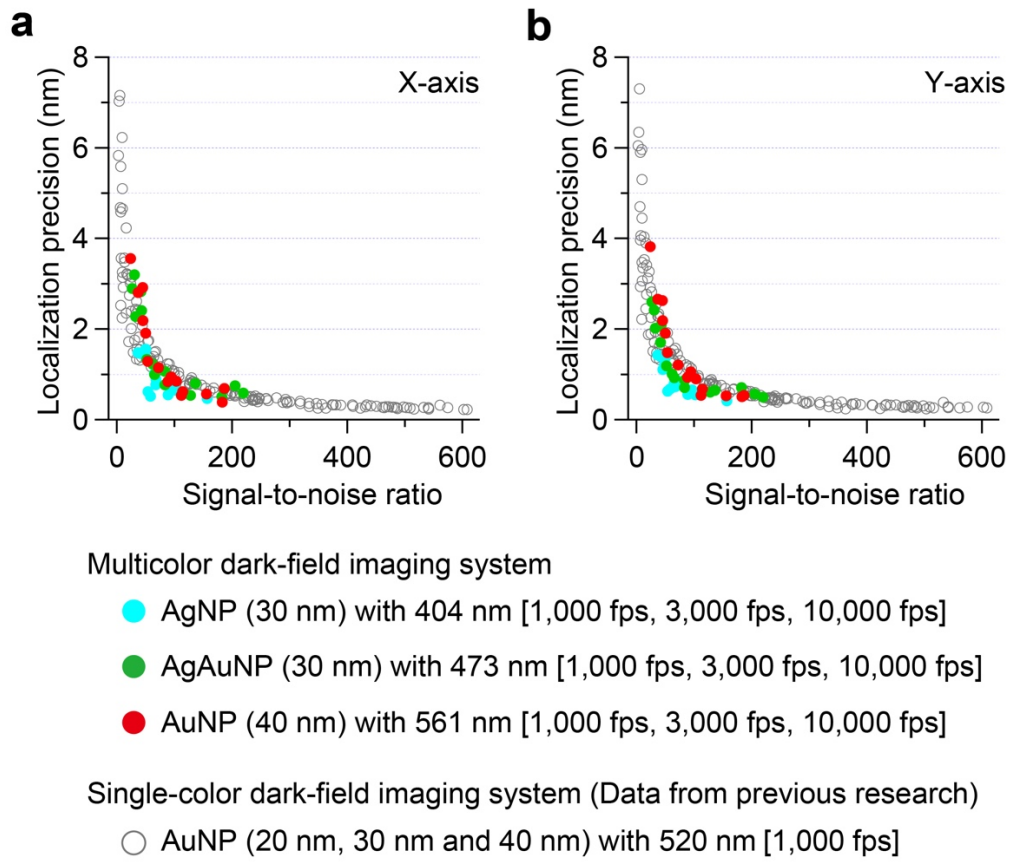

Figure S2. Relationships between localization precision and signal-to-noise ratio (S/N) of metal NPs obtained by the multicolor or single-color dark-field imaging system. (**a, b**) Relationships between localization precision and S/N of metal NPs along the (**a**) X- and (**b**) Y-axes. Dark-field images of 30 nm AgNPs, 30 nm AgAuNPs (5:5), and 40 nm AuNPs were obtained by spectrometer-based multicolor dark-field imaging system with 404 nm, 473 nm, and 561 nm lasers. The images were taken at 1,000, 333, and 100 μs time resolution (1,000 fps, 3,000 fps, and 10,000 fps), respectively. Dark-field images of 20 nm, 30 nm, and 40 nm AuNPs were obtained by single-color dark-field imaging system with 520 nm laser, as reported previously[1]. The images were taken at 1,000 μs time resolution (1,000 fps). Localization precision and S/N of each metal NP was calculated, and plotted.

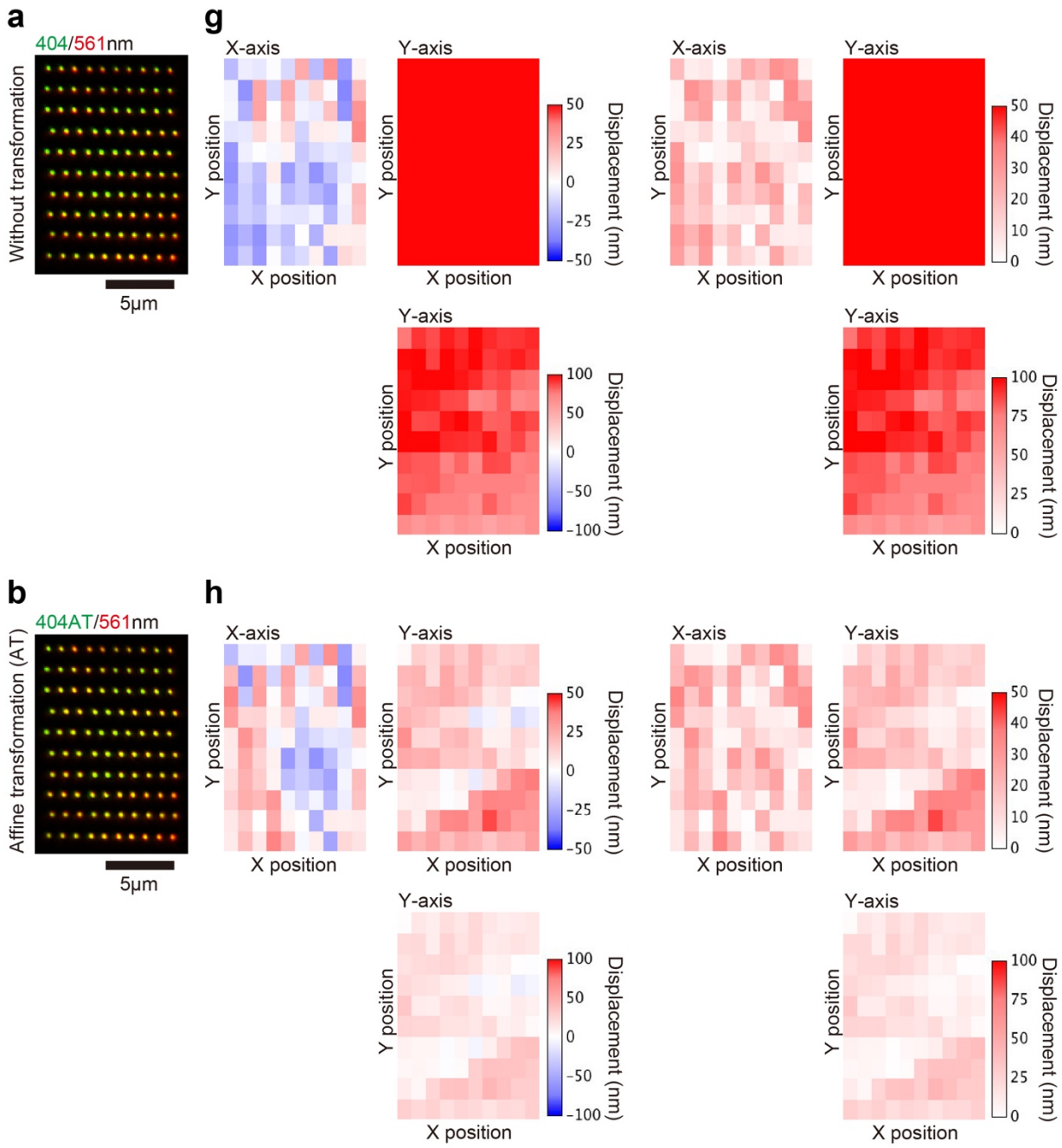
a
404/561nm
Without transformation
5μm
g
X-axis
Y-axis
Y position
X position
Displacement (nm)
50
25
0
−25
−50
100
75
40
30
20
10
b
404AT/561nm
Affine transformation (AT)
h

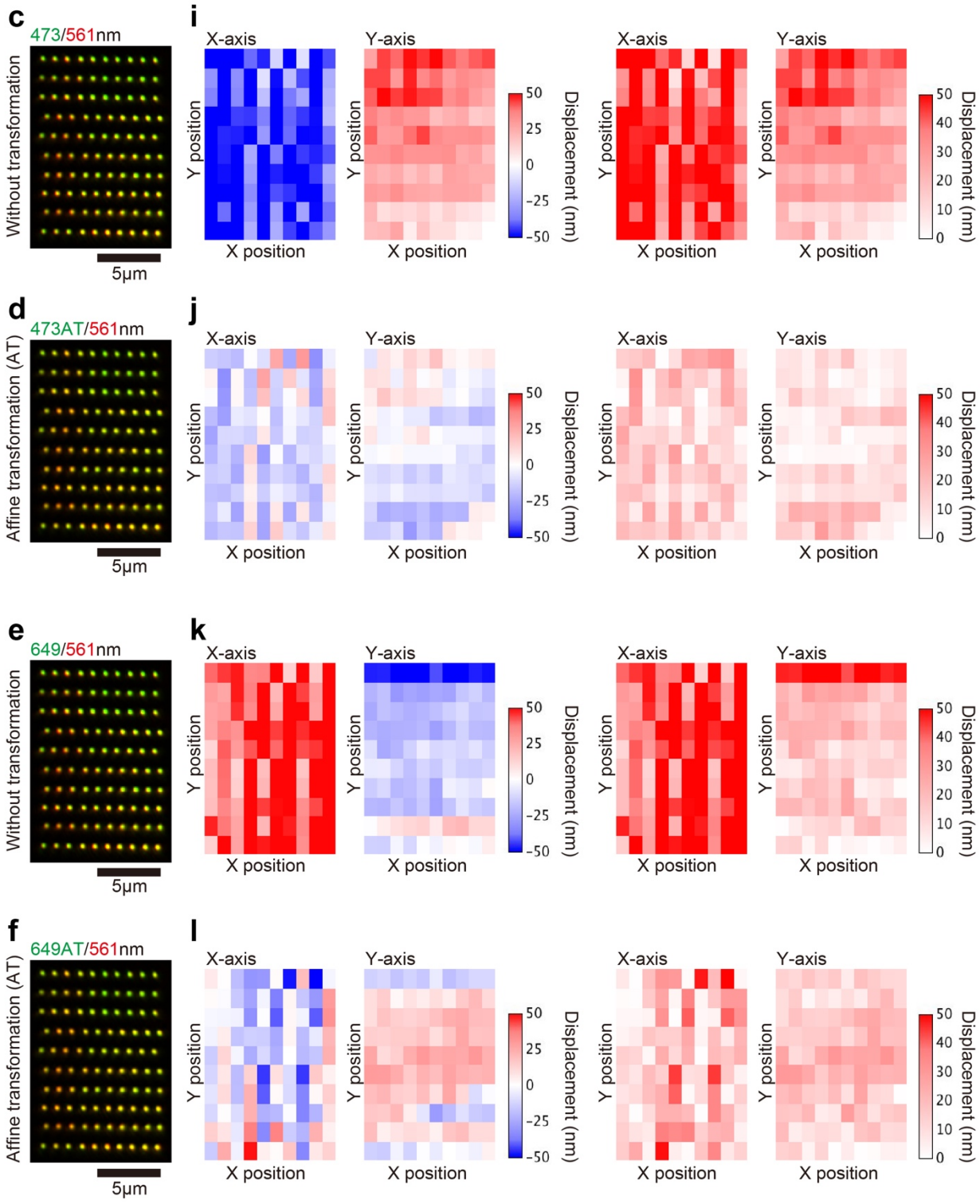
c
473/561nm
Without transformation
5μm
i
X-axis
Y-axis
Y position
X position
Displacement (nm)
50
25
0
-25
-50
40
30
20
10
d
473AT/561nm
Affine transformation (AT)
j
e
649/561nm
k
f
649AT/561nm
l

Figure S3. Spatial distribution of the positional shifts of the center position of an AuNP in four color channels without and with affine transformation. (**a-f**) Dark-field images of 50 nm AuNP, taken by spectrometer-based multicolor imaging system with 404 nm, 473 nm, 561 nm, and 649 nm lasers, without (a, c, e) and with affine transformation (b, d, f). The AuNP was two-dimensionally scanned to form 10 × 10 array. The image was taken at 1,000 μs time resolution. Each dark-field image shows maximum intensity projection of the snapshot of AuNP image at different 100 locations. Dark-field image at 561 nm was overlaid with the image at (a) 404 nm, (b) 404 nm with affine transformation, (c) 473 nm, (d) 473 nm with affine transformation, (e) 649 nm, and (f) 649 nm with affine transformation. Laser intensities were 4.4 $\mu W/\mu m^2$ for 404 nm, 4.1 $\mu W/\mu m^2$ for 473 nm, 1.5 $\mu W/\mu m^2$ for 561 nm, and 3.9 $\mu W/\mu m^2$ for 649 nm. Scale bar, 5 μm. (**g-l**) Spatial distributions of the values and absolute values of the positional shifts of the center positions of AuNP between (e) 561 nm and 404 nm, (f) 561 nm and 404 nm with affine transformation, (g) 561 nm and 473 nm, (h) 561 nm and 473 nm with affine transformation, (i) 561 nm and 649 nm, and (j) 561 nm and 649 nm with affine transformation.

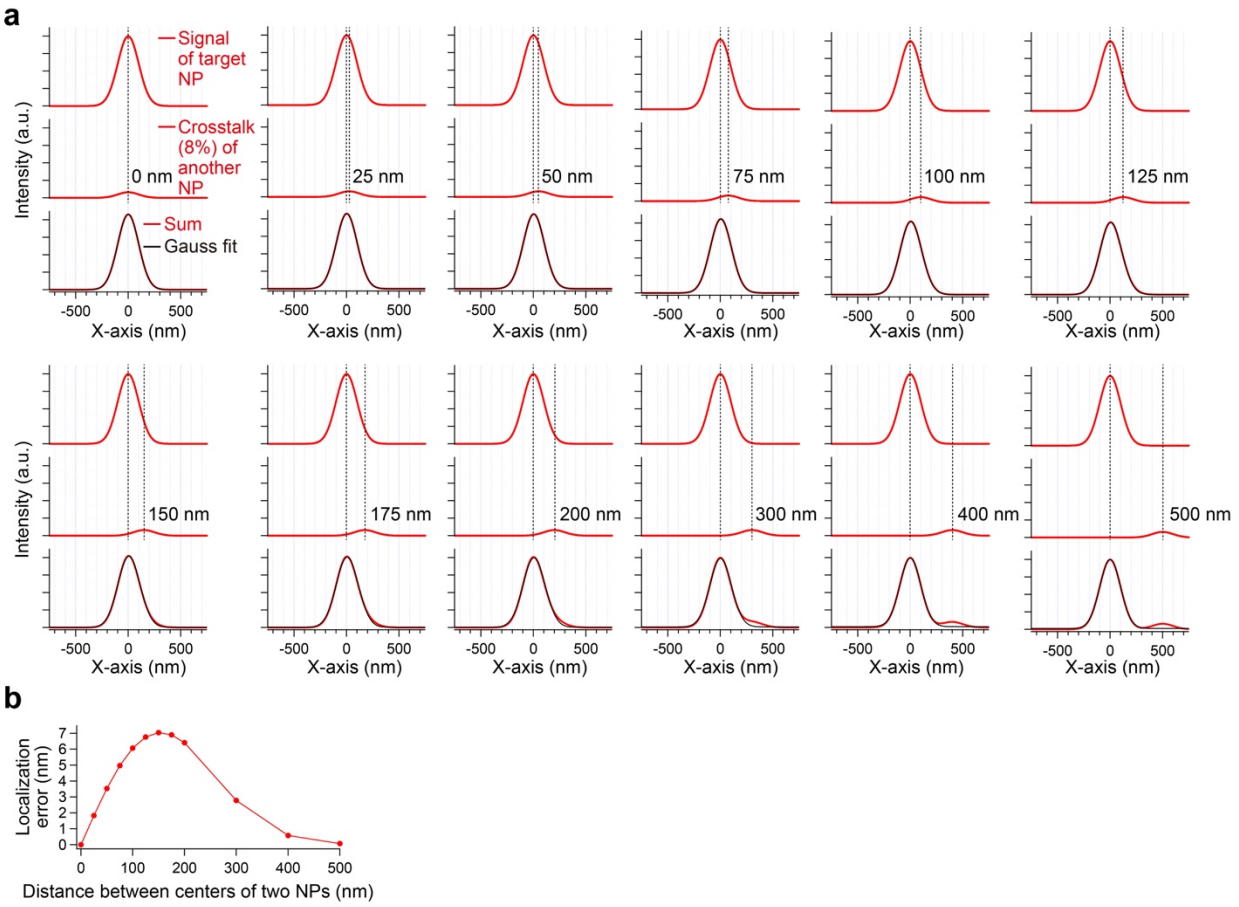

Figure S4. Estimation of the effect of crosstalk on localization accuracy. **(a)** Gaussians with SD of 100 nm were plotted to represent the line profile of the dark-field image of target NP. Another Gaussians with SD of 100 nm were also plotted with 8% intensity of the target NP to represent the line profile of the crosstalk from another NP. The distance of their center positions was changed from 0 nm to 500 nm. Sums of two line profiles (target NP and crosstalk) were plotted and analyzed with Gaussian fit. **(b)** Displacement of the center position (localization error) of summed profile from that of original profile without crosstalk plotted as a function of distance between center positions of two NPs.

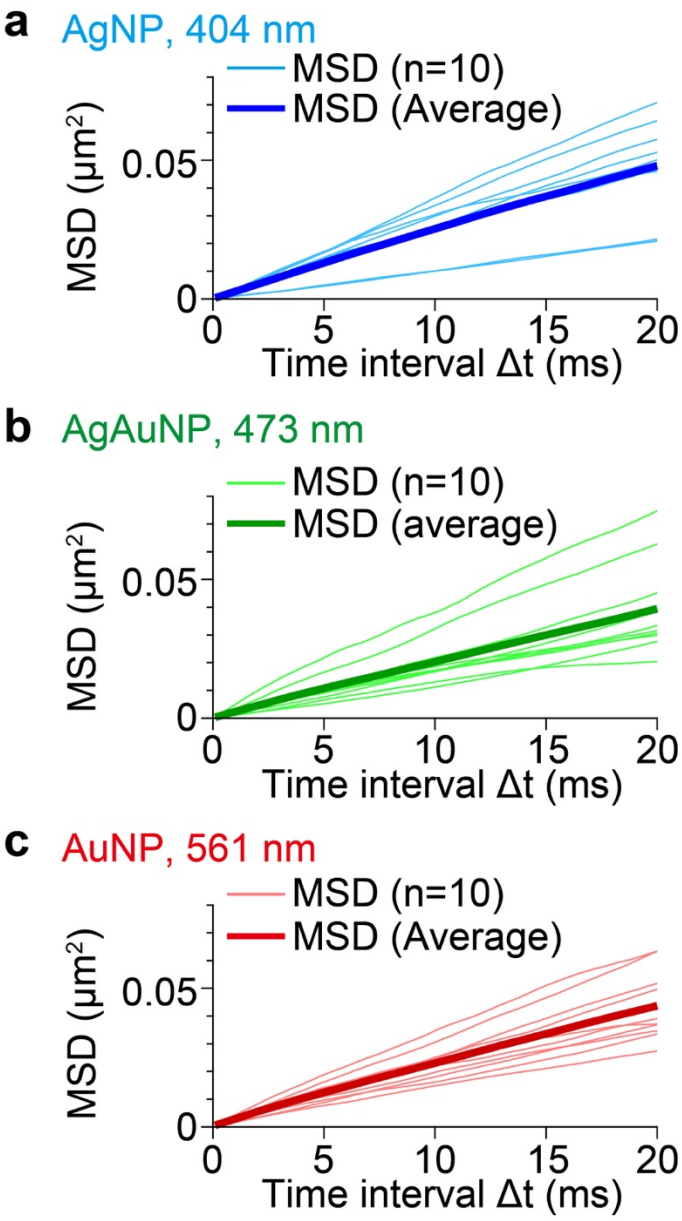

Figure S5. MSD plots of metal NPs attached to phospholipids in a supported membrane. MSD plots of the trajectory of (**a**) 30 nm AgNPs, (**b**) 30 nm AgAuNPs, and (**c**) 40 nm AuNPs. Time resolution of the measurement was 100 μs. For each metal NP, 10 trajectories with 1,800 frames were analyzed. MSD plots for AgNPs, AgAuNPs, and AuNPs were shown with light cyan, light green, and light red colors, respectively. Averaged MSD plots for AgNPs, AgAuNPs, and AuNPs were shown as cyan, green and red colors, respectively.

Table S1. Actual diameters and hydrodynamic diameters of 30 nm AgNPs, 30 nm AgAuNPs (5:5), and 40 nm AuNPs obtained by electron microscopy and dynamic light scattering measurements.

Electron microscope	AgNPs	AgAuNPs (5:5)	AuNPs
Actual diameters (nm) [a]	28.5 ± 4.4	31.5 ± 5.7	39.9 ± 3
n	684	460	213

Dynamic light scattering	AgNPs		AgAuNPs (5:5)		AuNPs	
Surface modification	Bare	Modified [c]	Bare	Modified	Bare	Modified
Hydrodynamic diameters (nm) [b]	37.4 ± 1.4	39.9 ± 1.7	45.6 ± 1.5	48.1 ± 2.0	43.3 ± 1.3	46.7 ± 1.2
n	20	20	20	20	20	20

a. The averages and standard deviations of the actual diameter of each metal NP are displayed. The actual diameters were calculated from the cross-section area of metal NPs in electron microscope image with the assumption that they have spherical shape.

b. The averages and standard deviations of the hydrodynamic diameter of each metal NP, without and with surface modification, are displayed. The hydrodynamic diameters were calculated from the cumulant fit to the autocorrelation function in dynamic light scattering measurement.

Table S2. Crosstalks of dark-field images of AgNPs, AgAuNPs (5:5), and AuNPs in four wavelength channels without pixel intensity offset.

Channel	404 nm	473 nm	561 nm	649 nm
30 nm AgNPs	100%[a]	23.6%	7.2%	5.5%
30 nm AgAuNPs (5:5)	12.9%	100%	17.9%	10.5%
40 nm AuNPs	19.7%	29.6%	100%	29.2%

a. The method for intensity calculation was same as Table 1.

Table S3. Diffusion coefficient and anomalous exponent of streptavidin-coated 30 nm AgNPs (404 nm), 30 nm AgAuNPs (5:5) (473 nm), and 40 nm AuNPs (561 nm) attached to biotinylated phospholipids in a supported membrane.

Metal NPs (Channel)	30 nm AgNPs (404 nm)	30 nm AgAuNPs (5:5) (473 nm)	40 nm AuNPs (561 nm)
Diffusion coefficient D ($\mu m^2/s$)[a]	0.60 ± 0.21[b] [0.59 ± 0.20] [c]	0.48 ± 0.21 [0.49 ± 0.21]	0.53 ± 0.16 [0.54 ± 0.17]
Anomalous exponent α	0.93 ± 0.12 [0.92 ± 0.14]	0.95 ± 0.21 [0.95 ± 0.24]	0.93 ± 0.14 [0.93 ± 0.17]

a. MSD plots in Figure S5 were fitted to an anomalous diffusion model to calculate diffusion coefficient D ($\mu m^2/s$) and anomalous exponent (α). First 200 data points of MSD plots which corresponds to a time interval from 100 μs to 20 ms, were used for calculation.

b. Each column shows average ± standard deviation of diffusion coefficient or anomalous exponent of all trajectories (n = 10 metal NPs for each condition).

c. Values in brackets show average ± standard deviation of diffusion coefficient or anomalous exponent of all trajectories with 10 times reduced sampling rate (equivalent to time resolution at 1,000 μs). First 20 data points of MSD plots, which corresponds to a time interval from 1000 μs to 20 ms, were used for calculation.

Movie S1. Movie of the merged dark-field images of 30 nm AgNPs (cyan, 404 nm), 30 nm AgAuNPs (green, 473 nm), and 40 nm AuNPs (red, 561 nm) attached to biotinylated phospholipids in a supported membrane. The images were taken at 100 μs time resolution with duration of 0.18 s (1800 frames in total). The movie was replayed at 200 frames per second. Image size is 8.0 μm × 10.3 μm. Pixel intensity offset was 15% of the highest pixel value of the reference NP images.

Movie S2. Movie of the dark-field images of a 30 nm AgAuNP (5:5) and a 40 nm AuNP attached to biotinylated phospholipids in a supported membrane. The top is a merged image sequence at 473 nm channel (green, 30 nm AgAuNP (5:5)) and 561 nm channel (red, 40 nm AuNP). The bottom is an image sequence at 649 nm channel (gray, plasmon coupling). The images were taken at 100 μs time resolution with duration of 32.7 ms (327 frames in total). The movie was replayed at 50 frames per second. Image size is 2.3 μm × 2.3 μm for both top and bottom of the movie. Pixel intensity offset was 15% of the highest pixel value of the reference NP images.

Movie S3. Movie of the merged dark-field images of 30 nm AgNPs (cyan, 404 nm channel), 30 nm AgAuNPs (5:5) (green, 473 nm channel), and 40 nm AuNPs (red, 561 nm channel) attached to kinesin-1 heads at 100 μs time resolution and 1 mM ATP. The images were taken with duration of 5.92 s (59,160 frames in total). The frame number of the movie was 10 times reduced, and the movie was replayed at 200 frames per second. Image size is 11.2 μm × 23.8 μm. Pixel intensity offset was 15% of the highest pixel value of the reference NP images. Rectangles in the

movie (cyan for AgNP, green for AgAuNP, and red for AuNP) indicate locations of each metal NP, which was analyzed in Figure 7.

REFERENCES

1. Ando, J.; Nakamura, A.; Visootsat, A.; Yamamoto, M.; Song, C.; Murata, K.; Iino, R. Single-Nanoparticle Tracking with Angstrom Localization Precision and Microsecond Time Resolution. *Biophys. J.* **2018,** *115* (12), 2413−2427.